Synergistic Effects in Ultrafine Amorphous InS_xO_y Nanowires Boost Photocatalytic Syngas Production from CO_2

Zejun Zhao[a]‡, Zailun Liu[b,c]‡, Yong Yang[a,*], Teng Wang[a], Fei Teng[c], Wenjun Jiang[b,*], Junjun Li[d], Zhicheng Zhang[d,*]

[a] State Key Laboratory of Solidification Processing, Center of Advanced Lubrication and Seal Materials, Northwestern Polytechnical University, Xi'an, Shaanxi 710072, P. R. China

[b] Qian Xuesen Laboratory of Space Technology, China Academy of Space Technology, 104 Youyi Road, Beijing 100094, P. R. China

[c] School of Environmental Science and Engineering, Nanjing University of Information Science & Technology, Nanjing 210044, China

[d] Tianjin Key Laboratory of Molecular Optoelectronic Sciences, Department of Chemistry, School of Science, Tianjin University & Collaborative Innovation Center of Chemical Science and Engineering, Tianjin 300072, China

*Corresponding author:
yongyangfj@nwpu.edu.cn; jiangwenjun@qxslab.cn; zczhang19@tju.edu.cn

Experiment section

1. Chemicals

Indium(III) chloride tetrahydrate ($InCl_3 \cdot 4H_2O$) was purchased from Tianjin Kemeiou Chemical Reagent Co. LTD. Thiourea (CH_4N_2S) was purchased from Shanghai Huzhou Chemical Co. LTD. Terpineol was obtained from Aladdin Chemical Reagent Company. Oleylamine (C18:90%) was purchased from Beijing Innochem Science & Technology Co. LTD.

2. Preparation of photocatalysts

2.1 Synthesis of the ultrathin InS_xO_y nanowires.

Typically, 58.6 mg of indium chloride tetrahydrate and 11.4 mg of thiourea were dissolved in a mixed solution containing 5.0 mL of ethanol and 5.0 mL of terpineol. Then, 2.0 mL of oleylamine was added into above solution resulting a transparent solution after stirring. Finally, the obtained solution was transformed into 25.0 mL Teflon-sealed autoclave and heated at 200 °C for 6 h. The products were collected by physical centrifuging at 8000 rpm, washed with 5.0 mL hexamethylene and 10.0 mL ethanol for several times.

2.2 Synthesis of the ultrathin InS_xO_y nanosheets.

58.6 mg of indium chloride tetrahydrate and 38.0 mg of thiourea were dissolved in a mixed solution containing 5.0 mL of ethanol and 5.0 mL of terpineol. Then, 2.0 mL of oleylamine was added into above solution resulting a transparent solution after stirring. Finally, the obtained solution was transformed into 25.0 mL Teflon-sealed autoclave and heated at 200°C for 6 h. The products were collected by physical centrifuging at 8000 rpm, washed with 5.0 mL hexamethylene and 10.0 mL ethanol for several times.

2.3 Synthesis of the In_2O_3 nanospheres.

58.6 mg of indium chloride tetrahydrate was dissolved in a mixed solution containing 5.0 mL of ethanol and 5.0 mL of terpineol. Then, 2.0 mL of oleylamine was added into above solution resulting a transparent solution after stirring. Finally, the obtained solution was transformed into 25.0 mL Teflon-sealed autoclave and heated at 200 °C for 6 h. The products were collected by physical centrifuging at 8000 rpm, washed with

5.0 mL hexamethylene and 10.0 mL ethanol for several times.

3. Materials Characterization

The structures, morphologies, chemical compositions and distribution and the phase composition of the as-prepared products were investigated by TEM, STEM, EDS Mapping, XPS, and XRD techniques. Powder X-ray diffraction (XRD) spectra was recorded by using a Rigaku D/Max 2500 diffractometer with Cu Kα radiation in the range of 2θ = 10°-80°. X-ray photoelectron spectroscopy (XPS) tests were carried out on the PHI5000VersaProbe III instrument, aiming to analyze chemical elements' composition of the preparative samples qualitatively and quantitatively. The microstructure was examined by transmission electron microscopy (TEM) (JEOL-JEM-2010) at an operation voltage of 200 kV. Inductively coupled plasma atomic emission spectroscopy (ICP-AES) was used to analyze the element contents of the products. The ultraviolet photoemission spectroscopy (UPS) was measured by a Thermo Fisher 250Xi instrument with a photon energy of 21.22 eV, the contact potential difference between the samples and the spectrometer was estimated using the formula $E_{NHE}/V = \Phi + VB_{max} - 4.44$ (E_{NHE}: potential of normal hydrogen electrode at pH = 0; Φ: the electron work function of the spectrometer). The In-situ FT-IR spectra were acquired from a Shimadzu Tracer-100 FTIR spectrometer.

4. Photoelectrochemical measurements

The electrochemical measurement of as-prepared sample was performed on an electrochemical workstation (Bio-Logic VSP). The electrochemical impedance spectroscopy (EIS), and photocurrent response were performed by using three-electrode measurement method, that is, the Ag/AgCl electrode was used as reference electrode, the Pt wire conduct as counter electrode, the 0.5 M Na_2SO_4 served as electrolyte solution, and the catalysts powder coated on the FTO glass sbustrate was served as working electrode. 5 mg of sample was added in 0.5 mL ultra-pure water, and dispersed the sample to form a homogeneous slurry by ultrasonic method. After 60 min, the homogeneous slurry was dispersed on the FTO glass sbustrate (1 cm × 1 cm) and dried at room temperature. The light source is the 300 W Xe lamp (Perfect Light, China).

4.1 Fluorescence Lifetime measurements

Time-resolved fluorescence spectroscopy of as-prepared samples were obtained from the Edinburgh Instruments FLS980 (λex = 325 nm, λem = 450 nm) and the decay curves can be well fitted by the following biexponential equations:

$$\tau = \frac{\sum A_n \tau_n^{\ 2}}{A_n \tau_n} \quad \text{(n=1,2,3.....)} \tag{1}$$

$$y = y_0 + \sum A_n e^{-x/\tau_n} \quad \text{(n=1,2,3.....)} \tag{2}$$

where the y_0 represents the baseline correction value, A_n (n=1,2,3.....) are the pre-exponential factors, and τ_n (n=1,2,3.....) and τ represent the lifetime (ns) in different processes and average lifetime.

4.2 Photocatalytic CO_2 reduction

The CO_2 photoreduction activity evaluation of as-prepared samples was conducted by a 120 mL PLR MFPR-I closed gas system (Perfect Light, China). The light source is the 300 W Xe lamp (Perfect Light, China). Typically, 4 mg of sample, 5 mg of $CoCl_2$, 15 mg of 2'2-bipyridine (bpy), 1 mL of triethanolamine (TEOA), 2 mL of H_2O and 3 mL of acetonitrile (MeCN) were added into a 120 mL PLR MFPR-I closed gas system. Subsequently, the reaction vessel was vacuum-treated and pumped by high-purity CO_2 (99.99%) for five times, then make the CO_2 to reach an atmospheric pressure. A 300 W Xe lamp light source directly irradiated the photocatalysts through the quartz window of reaction vessel. The products were determined by online analysis method using gas chromatography (GC2002, Ke Chuang Corp., China), equipping with a flame ionization detector (FID).

The cobalt phthalocyanine (CoPc) as cocatalyst for CO_2 photoreduction is according to the reported literature method. Typically, 4 mg as-prepared sample, 3 mg CoPc, 3 mL ultra-pure water, 1 mL TEOA, and 1 mL acetonitrile were added into the reaction vessel. Subsequently, the reaction vessel was vacuum-treated and pumped by high-purity CO_2 (99.99%) for five times, then make the CO_2 to reach an atmospheric pressure. A 300 W Xe lamp light source directly irradiated the photocatalysts through the quartz window of reaction vessel. The next steps are the same as the above

$Co(bpy)_3^{2+}$ as CO_2 reduction cocatalysts.

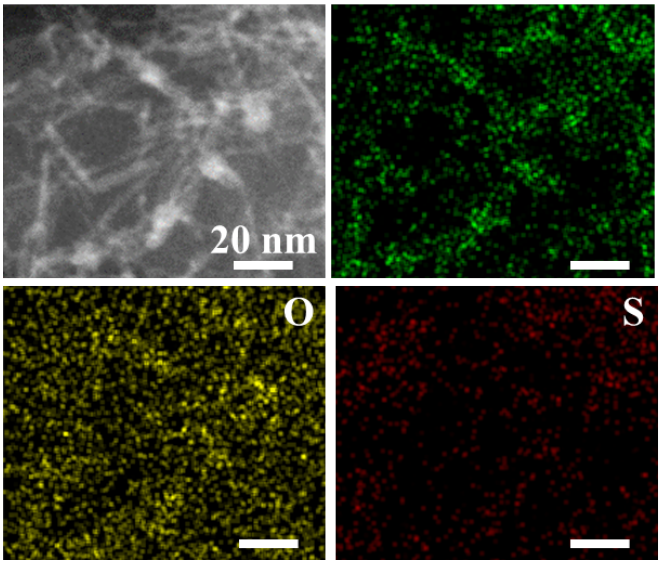

Figure S1. EDS mapping images of S, O, and In elements.

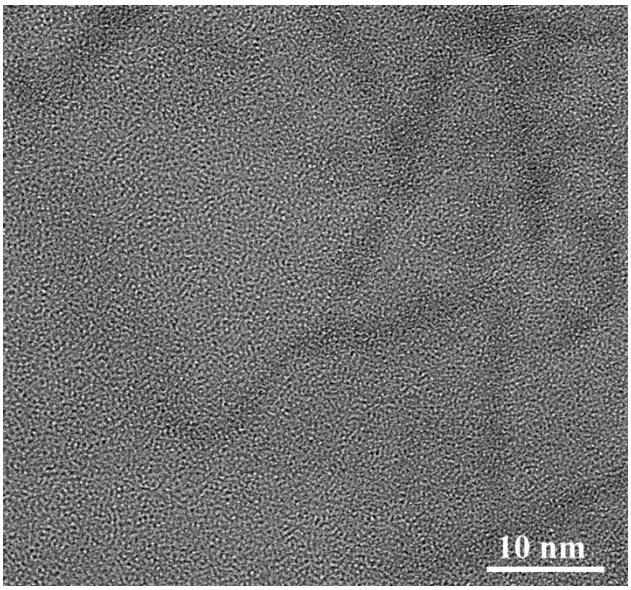

Figure S2. HRTEM image of InS_xO_y NWs.

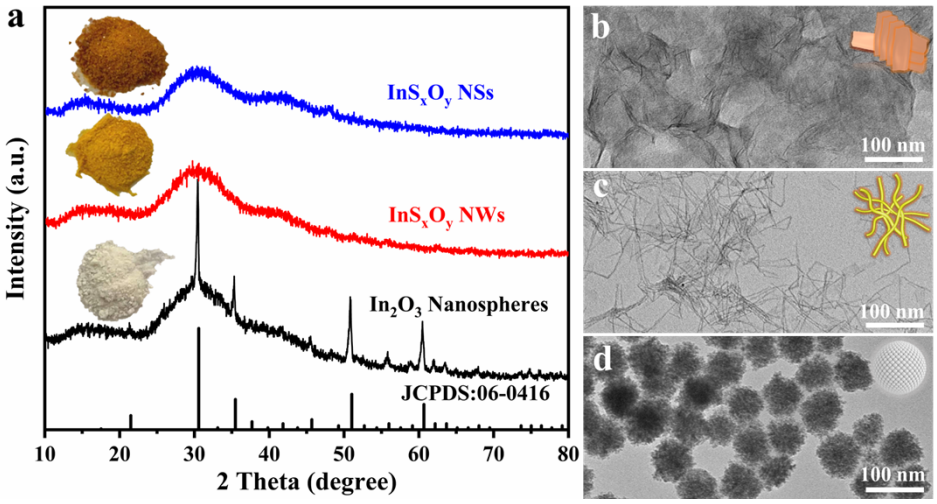

Figure S3. (a) The XRD patterns of In_2O_3 nanospheres, InS_xO_y NWs and InS_xO_y NSs. (b-d) TEM images of InS_xO_y NSs, InS_xO_y NWs and In_2O_3 nanospheres.

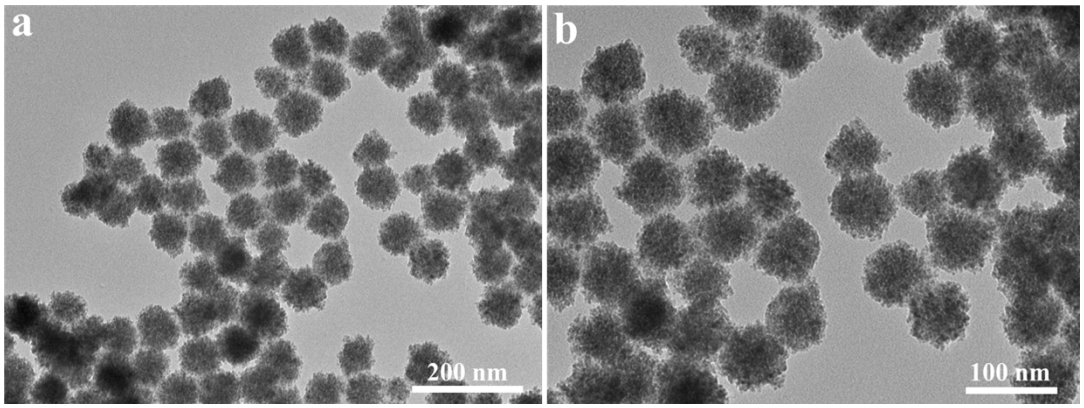

Figure S4. (a-b) TEM images of pure In_2O_3 nanospheres.

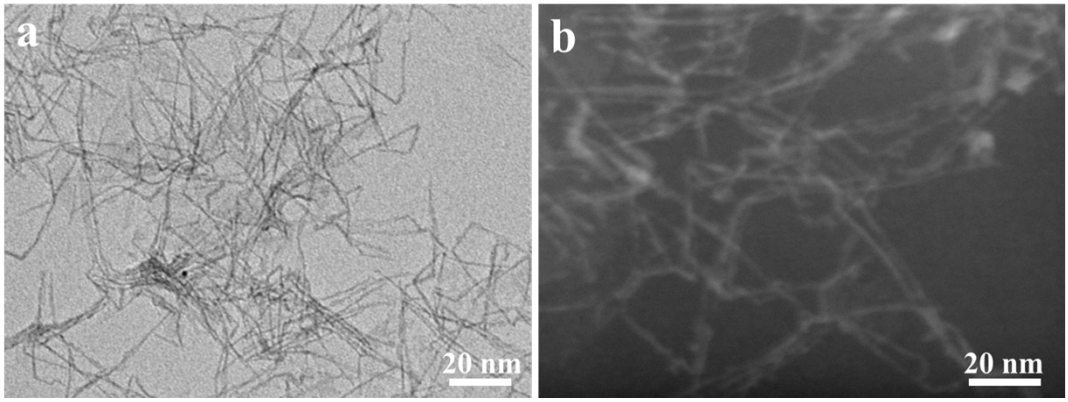

Figure S5. (a) TEM image of InS_xO_y NWs, (b) HAADF-STEM image of InS_xO_y NWs.

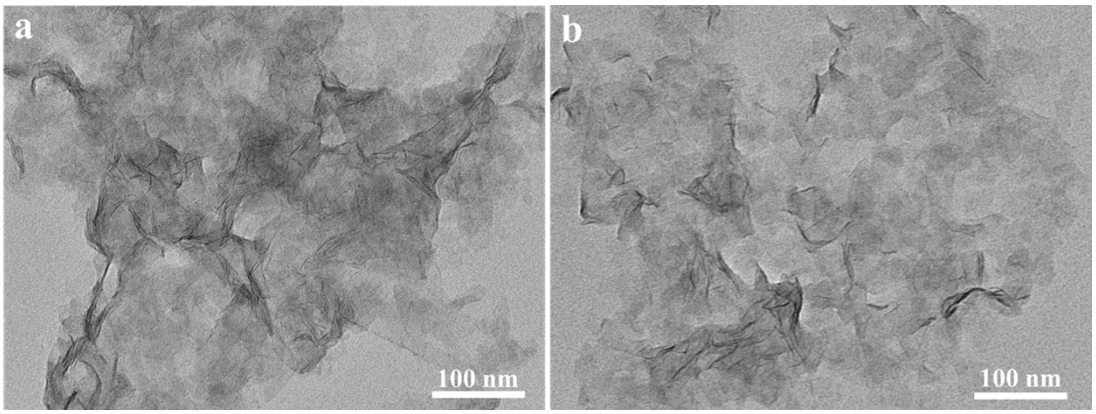

Figure S6. (a-b) TEM images of InS_xO_y NSs.

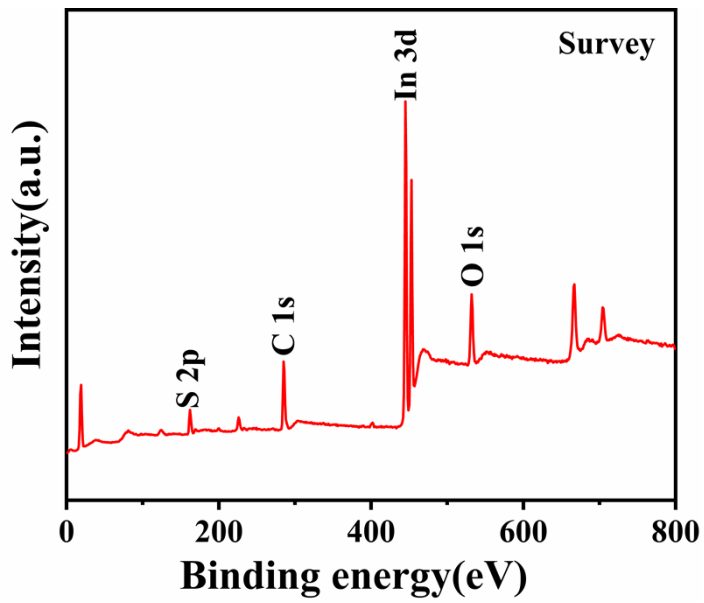

Figure S7. XPS survey spectrum of the InS_xO_y NWs.

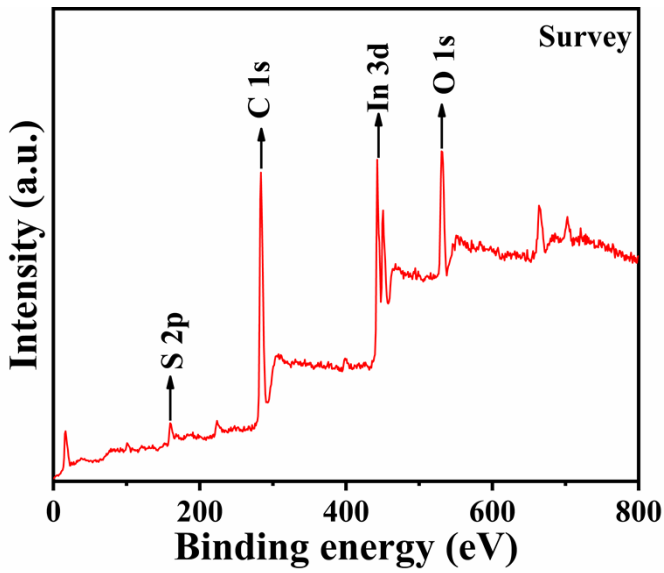

Figure S8. XPS survey spectrum of the InS_xO_y NSs.

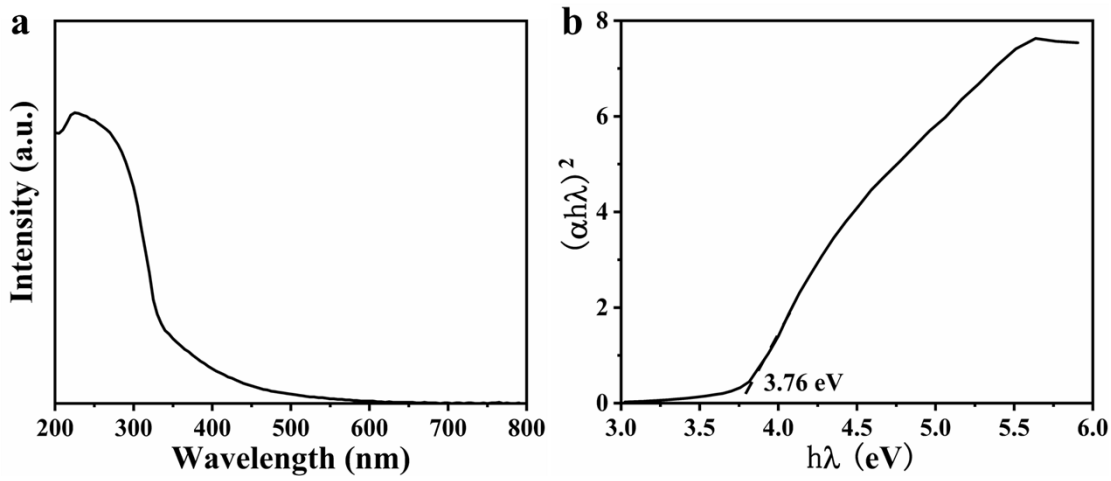

Figure S9. (a) UV-vis diffuse reflectance spectra and (b) plots of the transformed Kubelka-Munk function versus the light energy.

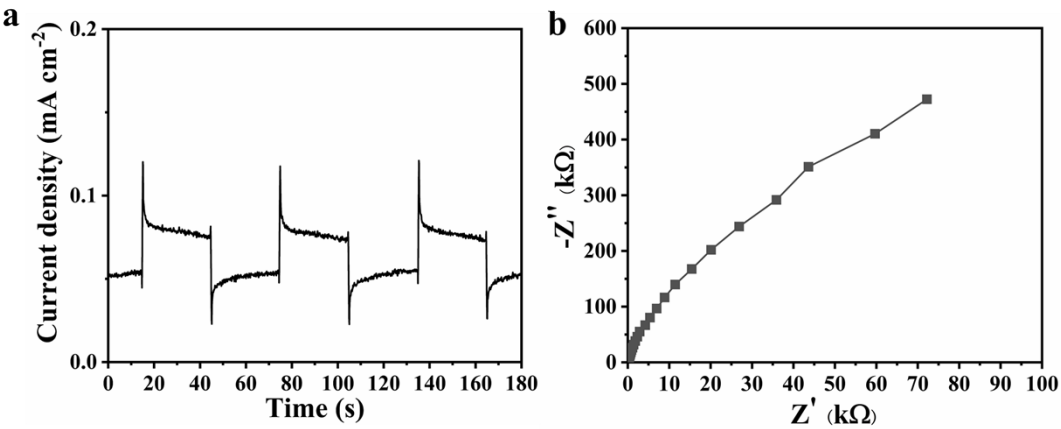

Figure S10. (a) Photocurrent response curves of In_2O_3 nanospheres, and (b) Electrochemical impedance spectrum.

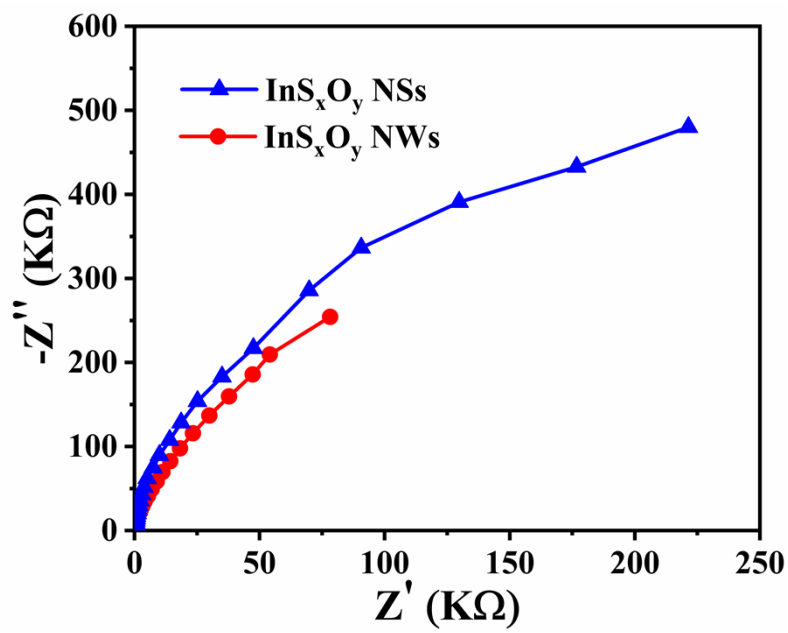

Figure S11. Electrochemical impedance spectra of InS_xO_y NSs and InS_xO_y NWs.

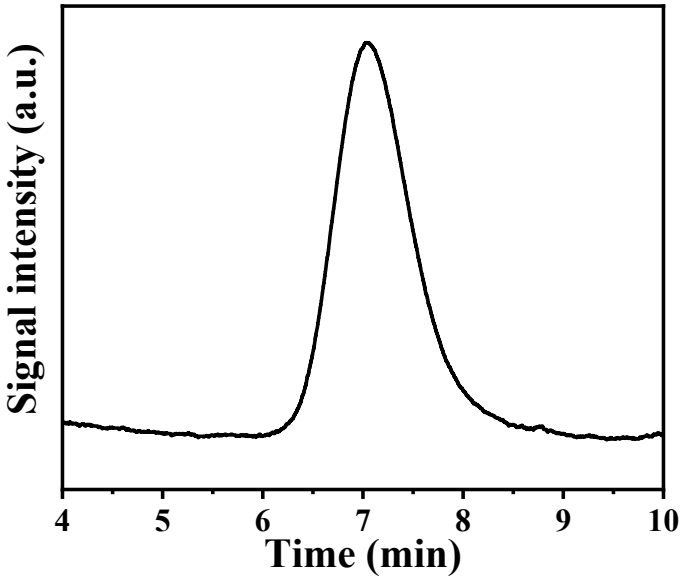

Figure S12. The CO peak of FID signal for InS_xO_y NWs photocatalytic CO_2 reduction system after 6 hours.

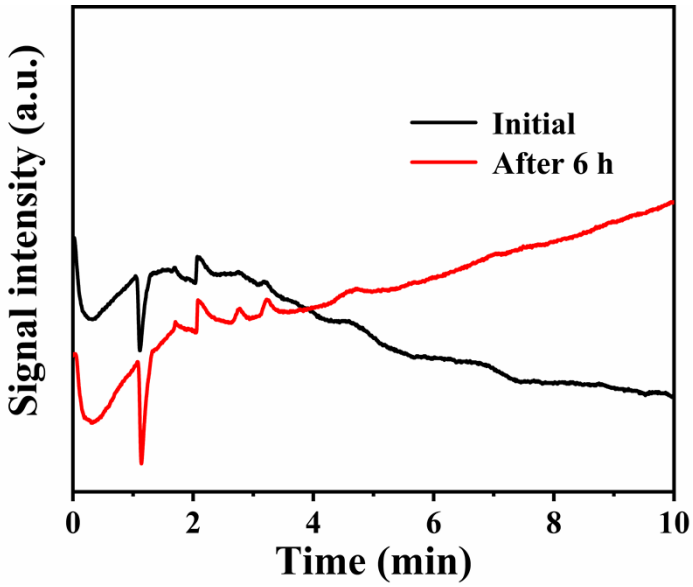

Figure S13. Gas chromatography spectra of photocatalytic CO_2 reduction without adding the photocatalysts.

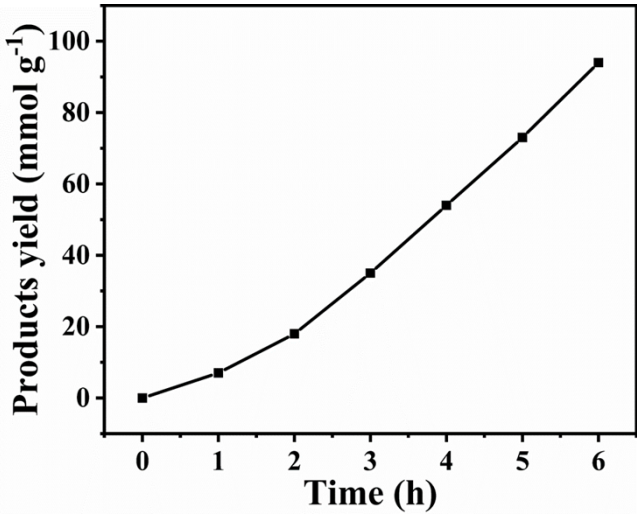

Figure S14. Photocatalytic CO_2 reduction performance of pure In_2O_3 nanospheres with the cocatalyst of $Co(bpy)_3^{2+}$.

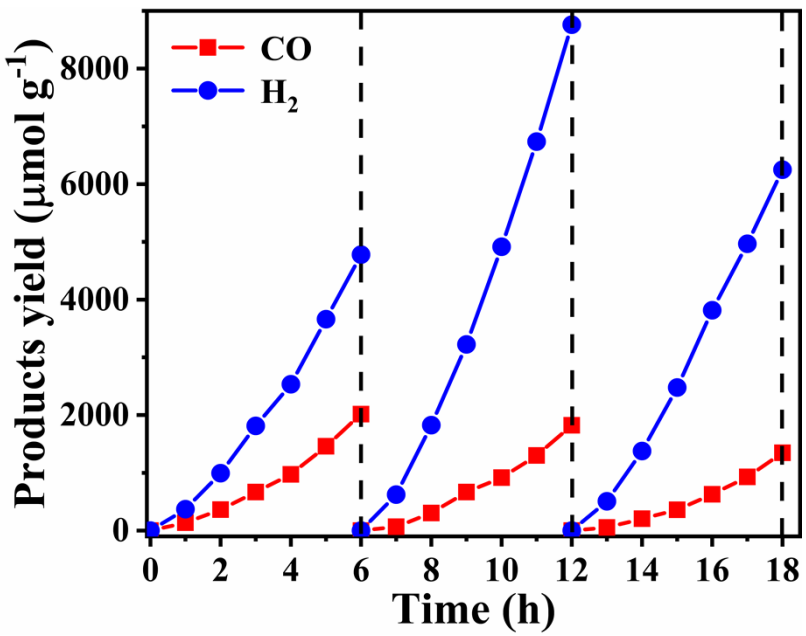

Figure S15. Cycling stability of InS_xO_y NWs.

Table S1. Band gap and energy band position of InS_xO_y NWs and InS_xO_y NSs.

Samples	Band gap (eV)	Valence band (eV)	Conduction band (eV)
InS_xO_y NWs	2.36	1.10	-1.26
InS_xO_y NSs	2.25	0.36	-1.89

Table S2. The fluorescence lifetime, time-resolved luminescence spectrum and polarization spectrum of the InS_xO_y NWs and InS_xO_y NSs.

Samples	**A_1**	**τ_1/ns**	**A_2**	**τ_2/ns**	**τ/ns**
InS_xO_y NWs	2896.10	7.37	1.64	80.67	7.82
InS_xO_y NSs	3187.10	7.046	1.76	70.46	7.39

Table S3. Comparison of the photocatalytic activity with other photocatalysts.

Photocatalyst	Synthesis methods	CO/H_2 production rates (μmol g^{-1} h^{-1})	Ref.
InS_xO_y NWs	**Solvothermal method**	**336/812**	**This work**
Pt/BP-OvMBWO Heterostructure	Hydrothermal method	20.5/16.8	ACS Appl. Mater. Inter. 2021, 13, 20162-20173.
MnO_x@TiO_2@CuPt	A hard-templating method	84.2/168.4	Chem. Sci. 2018, 9, 5334-5340.
Ni-SA-5/ZrO_2	Solvothermal method	11.8 (CO)	Adv. Energy Mater. 2020, 10, 2002928.
Br-Bi_2WO_6	Hydrothermal approach	13.8 (CO)	ChemSusChem, 2020, 13, 5638-5646.
$Co(OH)_2/H_2Ti_6O_{13}$ hybrid composite	Hydrothermal method	56.5/59.3	ACS Appl. Mater. Inter. 2021, 13, 38239-38247.
Co-Bi_3O_4Br	Hydrothermal method	107.1 (CO)	Nat. Commun. 2019, 10, 2840.
Atomically-thin Bi_2WO_6	Solvothermal method	75 (CO)	Angew. Chem. Inter. Ed., 2015, 54, 13971-13974.
$ZnIn_2S_4$	Solvothermal method	33.2 (CO)	J. Am. Chem. Soc., 2017, 139, 7586-7594.
CdSe QDs/ZnSe hybrid	Solvothermal method	25.6 (CO)	Chinese Chem. Lett. 2021, 32, 2474-2478
TiO_2-INA@CuP-Ph COF hybrid material	Solvothermal method	50.5 (CO)	J. Energy Chem. 2022, 64, 85-92.